

MOL #91751

Characterization of the novel positive allosteric modulator, LY2119620, at the muscarinic M₂ and M₄ receptors

Carrie H. Croy, Douglas A. Schober, Hongling Xiao, Anne Quets, Arthur Christopoulos, Christian C. Felder

Lilly Research Laboratories, Eli Lilly & Co., Lilly Corporate Center, Indianapolis, IN 46285, USA (C.H.C., D.A.S., H.X., A.Q., C.C.F)

[#]Monash Institute of Pharmaceutical Sciences and Department of Pharmacology, Monash University, Parkville, Victoria 3052, Australia (A.C.)

MOL #91751

Running Title: M₂/M₄ receptor modulation by LY2119620, ACh, Oxo and iperoxo

*Correspondence can be addressed to:

Christian C. Felder, Lilly Corporate Center, Indianapolis, IN 46285.

Phone: (317) 276-5384

Fax: (317) 276-7600

E-mail: felder@lilly.com

Number of text pages—30

Number of tables— 3

Number of figures— 5

Number of references – 44

Number of words in the Abstract— 250 words

Number of words in the Introduction – 599 words

Number of words in the Discussion – 1172 words

List of non-standard abbreviations: [³H]-NMS, [³H]-N-methylscopolamine; [³⁵S]-GTP-γ-S, guanosine 5'-[γ-³⁵S]-triphosphate; LY2119620, 3-amino-5-chloro-N-cyclopropyl-4-methyl-6-[2-(4-methylpiperazin-1-yl)-2-oxoethoxy] thieno[2,3-b]pyridine-2-carboxamide; LY2033298, 3-amino-5-chloro-6-methoxy-4-methyl-thieno(2,3-b)pyridine-2-carboxylic acid cyclopropylamide; GppNHp, guanosine-5'-(βγ-imido) triphosphate; iperoxo, [4-(4,5-dihydroisoxazole-3-yloxy)-but-2-ynyl]-N,N-dimethylamine; McN-A-343, 4-(N-(3-chlorophenyl)carbamoxyloxy)-2-butynyltrimethylammonium chloride; Oxotremorine M (Oxo-M); CHO, Chinese hamster ovary; PAM, positive allosteric modulator; receptor-G protein coupled state (RG); extracellular regulated kinase 1/2 (ERK1/2); glycogen synthase kinase 3b (GSK3B).

ABSTRACT

The M₄ receptor is a compelling therapeutic target as this receptor modulates neural-circuits dysregulated in schizophrenia, and there is clinical evidence that muscarinic agonists possess both anti-psychotic and pro-cognitive efficacy. Recent efforts have shifted toward allosteric ligands to maximize receptor selectivity and manipulate endogenous cholinergic and dopaminergic signaling. Here we present the pharmacological characterization of LY2119620, an M₂/M₄ receptor selective positive-allosteric modulator (PAM), chemically evolved from hits identified through an M₄ -allosteric functional screen. Though unsuitable as a therapeutic due to M₂ receptor cross-reactivity and thus potential cardiovascular liability, LY2119620 surpassed previous congeners in potency and PAM activity, and broadens research capabilities through its development into a radio-tracer. Characterization of LY2119620 revealed evidence of probe-dependence in both binding and functional assays. GTP- γ -S assays displayed differential potentiation depending on the orthosteric-allosteric pairing with the largest cooperativity observed for Oxo-M-LY2119620. Further [³H]-Oxo-M saturation binding, including studies with GppNHp, suggest that both the orthosteric and allosteric ligands can alter the population of receptors in the active G protein coupled state. Additionally, this work expands the characterization of the orthosteric agonist, iperoxo, at the M₄ receptor, and demonstrates that an allosteric ligand can positively modulate the binding and functional efficacy of this high efficacy ligand. Ultimately it was the M₂ receptor pharmacology and PAM activity with iperoxo which made LY2119620 the most suitable allosteric partner for the M₂ active-state structure recently solved (Kruse et al. 2013); a structure which provides crucial insights into the mechanisms of orthosteric activation and allosteric modulation of muscarinic receptors.

Introduction

Muscarinic acetylcholine receptors (mAChR, M₁ – M₅) regulate the action of the neurotransmitter acetylcholine, whose signaling roles in the CNS include modulation of processes of mood, cognition, exocrine gland function, and smooth muscle control (Wess et al. 2007; Young et al. 2010; Wess 2012). The demonstrated antipsychotic efficacy of muscarinic receptor agonists in both pre-clinical and clinical studies, make this G protein-coupled receptor (GPCR) subfamily attractive targets for the treatment of Alzheimer's disease and schizophrenia ((Bodick et al. 1997; Bymaster et al. 2002; Shekhar et al. 2008), reviewed in (Felder et al. 2012; Jones et al. 2012; McKinzie and Bymaster 2012)). A key bottleneck to research and therapeutic development efforts for the mAChR family has been the lack of receptor subtype-selective pharmacological tools to help determine the physiologic relevant family member(s) to target for various indications. However, over the past decade several muscarinic subtype-selective small molecule ligands have emerged through the successful targeting of unique allosteric binding sites generally located on the exterior surface loops of the receptors (example M₁ (Daval et al. 2013), M₂ (Huang et al. 2005), M₄ (Nawaratne et al. 2010), M₅ (Bridges et al. 2009)). Within this paper, we characterize the allosteric-site ligand LY2119620, and demonstrate that it is a high affinity M₂/M₄ receptor selective positive allosteric modulator (PAM).

LY2119620 was originally synthesized following hit expansion from a small-molecule screening effort for M₄ receptor-selective allosteric ligands beginning in 1998; a synthetic campaign that also resulted in LY2033298 built from the same thieno[2,3-b]pyridine core scaffold (Chan et al. 2004). After the 2004 patent filing by Eli Lilly (Esteban and Hillard May 2006), studies on molecules such as LY2033298 ((Chan et al. 2008; Nawaratne et al. 2008; Leach et al. 2010; Nawaratne et al. 2010; Leach et al. 2011; Suratman et al. 2011; Gannon and Millan 2012; Valant et al. 2012)) and others, e.g. VU10010 ((Brady et al. 2008; Shirey et al. 2008; Bridges et al. 2010; Lewis et al. 2010; Dencker et al. 2012; Salovich et al. 2012; Huynh et al. 2013; Le et al. 2013)), explored the SAR around this scaffold and the *in vivo* efficacy of such molecules in animal models. Concomitant structure-function work using methods such as site-

MOL #91751

directed mutagenesis have allowed the mapping of the various ligand binding sites to the M₄ receptor and in one instance, the M₂ receptor, and revealed critical regions involved in the receptor activation mechanism (Nawaratne et al. 2008; Nawaratne et al. 2010; Leach et al. 2011; Suratman et al. 2011; Valant et al. 2012). The resultant body of knowledge collected on this M₄ receptor-PAM scaffold over the past 15 years allowed us to successfully support the recent breakthrough crystallization efforts of M₂ receptor-active state structure (Kruse et al. 2013). Working from the necessity of finding an M₂ receptor selective-allosteric binder that could potentiate the already potent agonist, iperoxo, we undertook the characterization of the LY2119620 ligand. The advantage of this ligand over molecules such as LY2033298 was that it had greater M₂ receptor PAM activity when paired with ligands like Oxo-M. In the present work, we extend the preliminary pharmacological characterization of LY2119620 presented in the structural study (Kruse et al. 2013) to the study of all five muscarinic receptor subtypes, in both *in vitro* binding and G protein functional assays, to rigorously evaluate the pharmacology of LY2119620. These studies reveal LY2119620 to be: an M₂/M₄ receptor selective positive allosteric modulator of both orthosteric ligand binding and receptor-G protein signaling; display evidence of probe dependence (differences in cooperativity observed with different orthosteric-allosteric pairings); and positively modulate the potent muscarinic-agonist iperoxo at both the M₂ and M₄ receptor subtypes.

Materials and Methods

Materials CHO cell lines stably expressing human M₁ receptor (B_{max} NMS=4.4 pmol/mg membrane; Kd=0.35nM), M₂ receptor (B_{max} NMS =11.0 pmol/mg membrane; Kd=0.66nM), M₃ receptor (B_{max} NMS =7.64 pmol/mg membrane; Kd=0.30nM), M₄ receptor (B_{max} NMS =3.3 pmol/mg membrane; Kd=0.18nM) or M₅ receptor (B_{max} NMS =4.2 pmol/mg membrane; Kd=0.33nM) were purchased from Perkin Elmer (Waltham, MA). Chemical and ligands were obtained from the following sources: Guanosine-5'-[(β,γ)-imido]triphosphate (GppNHp) from Axxora (Farmingdale, NY); Oxotremorine-M (Oxo-M) from Tocris (Bristol, UK); Acetylcholine (ACh), from Sigma (St. Louis, MO); iperoxo from Eli Lilly or Monash Institute of Pharmaceutical Sciences (Melbourne, VIC, Australia); LY2119620 from Eli Lilly (Indianapolis, IN); [³H]-NMS from GE Healthcare (Piscataway, NJ); [³H]-LY2119620 from Vitrox (Placentia, CA); and [³H]-Oxo-M and [³⁵S] GTP-γ-S from Perkin Elmer (Waltham, MA). The chemical identity of LY2119620 is 3-amino-5-chloro-N-cyclopropyl-4-methyl-6-[2-(4-methylpiperazin-1-yl)-2-oxoethoxy] thieno[2,3-b]pyridine-2-carboxamide.

GTP-γ-[³⁵S] Binding Assays. The level of G protein activation was measured by the amount of non-hydrolyzable GTP-γ-[³⁵S] bound to G_{αi}- subunit. The GTP-γ-[³⁵S] binding was determined using a SPA-bead antibody capture technique (DeLapp et al. 1999). Note for the studies with iperoxo and the M₂ receptor a non-commercial membrane source was utilized; specifically 25 μg of the M₂ receptor P1 membrane preparations of a CHO cell line stably expressing human M₂ muscarinic receptor (B_{max}= 0.25 ± 0.007 pmol/mg membrane) were utilized. Otherwise 20 μg commercial M₁-M₅ receptor expressing membranes were utilized (Perkin Elmer). An EC₅₀ value for each response curve was determined by fitting the agonist response data to a three- or four-parameter fit model (GraphPad Prism). **Agonist-binding experiments.** For the agonist GTP-γ-[³⁵S] binding curves 20 μg of membranes were incubated in assay buffer (20 mM HEPES, 100 mM NaCl, 0.2 μM EDTA, 1 μM GDP and 10 mM MgCl₂, pH 7.4), 500 pM GTP-γ-[³⁵S], and varying concentrations of the orthosteric ligands (ACh, iperoxo, McN-A-343, and pilocarpine, or LY2119620) for 40 min at room temperature with mixing. The Gα-subunits were

MOL #91751

then captured using anti-rabbit-conjugated SPA beads (Perkin Elmer, 1.25mg/reaction), G α i antibody (Santa Cruz Biotechnologies, 1.3 μ g/reaction), and NP-40 (Roche, 0.1% final concentration) during a three hour room temperature incubation. The radioactivity counts of the bound GTP- γ -[³⁵S] were determined by scintillation spectrophotometry (Wallac Trilux, Perkin Elmer). An EC₅₀ value was determined by fitting the agonist response data using a three-parameter fit model (GraphPad Prism).

Interaction experiments. The GTP- γ -[³⁵S] binding experiment was run as above, except the orthosteric agonist concentration-response curve was measured in the presence of varying concentrations of allosteric ligand LY2119620 (0-10 μ M). EC₅₀ values at each concentration of LY2119620 were determined.

Allosteric EC50 Modulation Analysis. The ability of LY2119620 to act as an allosteric modulator was quantified by determining (i) the affinity of LY2119620 for the free receptor (K_B), and (ii) the magnitude and direction of the LY2119620's effect on a given orthosteric ligand's affinity by the co-operativity factor α (described in (Christopoulos and Kenakin 2002)). The K_B and α values was determined by fitting the eight dose-response curves (acquired in the presence of varying LY2119620 concentration) shown in each panel of Figure 3 to the "Allosteric EC50 shift" equation in GraphPad v6.7.

Radioligand Binding Assays. Binding assays were performed in 20 mM HEPES, 100 mM NaCl, 10 mM MgCl₂, pH 7.4 (binding buffer) unless noted. Studies were carried out using commercially prepared CHO membranes expressing the various muscarinic receptor subtypes (Perkin Elmer). Reactions were stopped by rapid filtration on a TOMTEC 96-well cell harvester (Tomtec; Hamden, CT). Non-specific binding was determined using 10 μ M atropine. Radioactivity retained on the filter-mat was counted on a scintillation spectrophotometry (Wallac 1205 Beta-plate, Perkin Elmer). Data were fit to appropriate models using GraphPad Prism 6.7 software (GraphPad Software, Inc.; San Diego, CA). [³H]-LY2119620

Saturation Binding Assays. [³H]-LY2119620 equilibrium binding was achieved by incubating 15 ug membranes, orthosteric ligand (100 μ M unless otherwise noted; Oxo-M, ACh, or iperoxo) and various concentrations of [³H]-LY2119620 (0.2-60 nM) for 1 h at 25 °C. Association kinetic experiments showed that [³H]-LY2119620 reached steady state within 15 minutes, however, a one hour incubation was used to

MOL #91751

allow all ligands within the reaction to reach equilibrium. The specific binding vs. time data was fit to a one-site specific binding model, and the Bmax and Kd for the allosteric molecule was calculated for each orthosteric ligand. **[³H]-Oxo-M Saturation Binding Assays.** [³H]-Oxo-M equilibrium binding experiments were a two-addition process achieved by: first pre-incubating 15 ug membranes and varying concentrations of [³H]-Oxo-M (0.05-15 nM) in the presence or absence of 100 μM GppNHp (GDP-nucleotide analog) for 30min at room temperature; then adding either 0 or 10μM allosteric ligand, LY2119620 for an additional 30 mins. The specific binding vs. time data was fit to a one-site specific binding model. **[³H]-NMS Kinetic Dissociation Experiments** The [³H]-NMS dissociation kinetic binding assays were performed using a reverse time protocol. Specifically, 10 μg of membrane, 0.2 nM [³H]-NMS, and varying concentrations of LY2119620 (0-40 μM, see Figure 5) were incubated for 1 hour at 30 °C in binding buffer. Once equilibrated, 1 μM iperoxo was added in a time-staggered approach to capture 1-90 minute time-points. The specific binding vs. time data was fit to a single exponential decay and the dissociation rate constant (min⁻¹) was determined for each concentration of LY2119620. **[³H]-[³H]-NMS Equilibrium Inhibition Binding Assays.** The displacement of [³H]-NMS was performed by adding iperoxo in the absence or presence 10 μM LY2119620. A concentration of 0.30 nM [³H]-NMS was incubated with 15 μg M₂/M₄ receptor-expressing membranes, 0 or 10 μM LY2119620, and varying concentrations of iperoxo (0-100 μM) and allowed to reach equilibrium for 2 h at 25 °C. The calculated Kd of [³H]-NMS was 0.348 nM for the M₂ receptor in the absence of LY2119620 and 0.402 nM in the presence of 10 μM LY2119620; the Kd was and 0.0878 nM and 0.109 nM for the M₄ receptor in the absence and presence of LY2119620, respectively (Supplemental Figure 2). The Cheng-Prusoff model was used to fit the K_i of iperoxo in the absence and presence of LY2119620 (Cheng and Prusoff 1973).

Results

Modulation of receptor-G protein coupled signaling by allosteric ligand, LY2119620.

To investigate the selective allosteric modulation of the M₂ and M₄ receptors we initially utilized receptor G protein coupled signaling at all muscarinic subtypes (M₁-M₅). As allosteric ligands such as LY2119620 (Figure 1) can demonstrate orthosteric probe-dependent binding (Kenakin 2007; Leach et al. 2010; Valant et al. 2012), studies were carried out in the presence of three orthosteric agonists, iperoxo, Oxo-M or ACh.

Characterization of high efficacy agonist, iperoxo, at the M₄ receptor. The agonist, iperoxo, has been reported to have both enhanced affinity and higher efficacy at the M₂ receptor compared to ACh (Langmead and Christopoulos 2013; Schrage et al. 2013). As this “super-agonism” had not been extensively explored at the M₄ receptor, concentration-response curves for the full-agonists ACh, Oxo-M, iperoxo and partial-agonist McN-A-343 were carried out using [³⁵S]-GTP-γ-S binding experiments. This assay format was used as it directly measures G protein activation, the first step in GPCR signal transduction. Oxo-M, ACh, and McN-A-343 were selected to calibrate the assay for exploration of the allosteric compound, LY2119620. The potencies of iperoxo at the M₂ receptor (2.12 ± 0.0953 nM) and at the M₄ receptor ($8.47\text{nM} \pm 3.00$ nM) are much greater than the respective EC₅₀ values of 118 ± 31.7 nM and 514 ± 22.0 nM observed for ACh. Under the conditions tested no differences in the maximal-response elicited by iperoxo, ACh or Oxo-M were observed (Figure 2).

Characterization of allosteric agonism of LY2119620 alone. Binding studies with a radio-labeled form of LY2119620, [³H]-LY2119620, showed no detectable binding of the molecule in the absence of orthosteric ligand at the M₁-M₅ receptor subtypes (Schober *et al.*, (companion manuscript)). The intrinsic agonist activity of LY2119620 was also assessed by running G protein activity assays. For these GTP-γ-S experiments membranes were incubated with LY2119620 in the absence of exogenous agonist, and the resultant concentration-response curves were normalized as a percentage of the maximal ACh response.

MOL #91751

As shown in Figure 2C, LY2119620 showed a modest allosteric agonism of $23.2 \pm 2.18 \%$ and $16.8 \pm 5.01 \%$ at the M_2 and M_4 receptors respectively. This agonism was less than that observed for the partial-agonist control compound McN-A-343 shown in Figure 2A. Minimal allosteric agonism (<20%) was observed for LY2119620 at the M_1 , M_3 , and M_5 receptors (Supplemental Figure 1). ***Characterization of allosteric modulation of orthosteric agonists, ACh, iperoxo, and Oxo-M by LY2119620.*** [^{35}S]-GTP- γ -S binding experiments were run to verify that LY2119620 potentiates the activity of an orthosteric agonist ligand, and to determine the degree of cooperativity between the orthosteric-allosteric sites. These experiments paired LY2119620 with agonists, ACh, Oxo-M or iperoxo, and were run at all muscarinic receptor subtypes (M_1 - M_5). The $M_1/M_3/M_5$ receptor subtypes showed minimal differences in EC_{50} values for all agonists tested (data for iperoxo and Oxo-M not shown; data for ACh shown in Supplemental Figure 1). Figure 3 shows positive cooperativity between LY2119620 and all agonists, with larger potentiation generally noted at M_4 than M_2 . These changes were quantified using the allosteric ternary complex model (Christopoulos and Kenakin 2002). The variable K_B estimates the affinity of LY2119620 for the allosteric binding site on the unoccupied receptor, and was found to be consistently be around 1.9-3.4 μM (insets Figure 3A-F). The cooperativity factor, α , which quantifies the affinity change of one ligand by the other ligand when both are bound to the receptor simultaneously, varied widely depending on the agonist-LY2119620 pairing. LY2119620 and ACh binding led cooperativity factors of 19.5 and 79.4 for the M_2 receptor and the M_4 receptor respectively (Figure 3A and 3B). The cooperativity factor of 79.4 at the M_4 receptor suggests that a higher degree of positive cooperativity exists between LY2119620 and ACh than the previously described allosteric $M_4 > M_2$ receptor modulator, LY2033298 (Chan et al. 2008; Nawaratne et al. 2010). The Oxo-M and LY2119620 pairing showed the highest degree of cooperativity with an alpha factor of 50.1 and 282 for the M_2 receptor and M_4 receptor respectively (Figure 3C and 3D). The iperoxo and LY2119620 pairing showed the most modest cooperativity with an α factor of 14.5 at the M_2 receptor and 3.9 at the M_4 receptor (Figure 3E and 3F). Additionally, unlike the other allosteric-orthosteric pairings (ACh and Oxo-M), LY2119620 showed a higher-degree of

cooperativity with iperoxo at the M₂ receptor rather than the M₄ receptor. Table 1 summarizes the agonist EC₅₀ values for each concentration of LY2119620 tested.

Ligand binding studies of LY2119620 to the M₂ and M₄ receptors

Saturation binding studies using both allosteric and orthosteric radio-ligands reveal probe dependence.

The functional GTP- γ -S binding experiments above establish that LY2119620 positively modulates the G protein coupled response of the M₂/M₄ receptor subtypes in a probe-dependent manner. To further elucidate this probe-dependence, we setup a series of saturation binding experiments to view these effects from both the allosteric and orthosteric ligand binding perspective. The [³H]-LY2119620 saturation binding allows assessment of probe-dependence from the allosteric site perspective to all three orthosteric ligands under identical experimental conditions. Detailed characterization of the LY2119620 allosteric radio-ligand, [³H]-LY2119620, is presented elsewhere (Schober et al. (companion manuscript)). The [³H]-LY2119620 saturation binding presented in Figure 4A and B show that the B_{max} values for the M₂ and M₄ receptors were highly agonist-dependent, while the K_d values displayed little variance. The B_{max} values at the M₂ receptor were over 10-fold higher for iperoxo (2640 ± 203 fmol/mg) and Oxo-M (2540 ± 353 fmol/mg) compared to ACh (160 ± 34.0 fmol/mg) (Figure 4A); the K_d values ranged from 11.2 ± 1.17 nM for iperoxo to 16.9 ± 0.700 nM for Oxo-M. Similarly, at the M₄ receptor the B_{max} for Oxo-M was 1110 ± 157 fmol/mg, which was significantly greater than both ACh (456 ± 55.0 fmol/mg) or iperoxo, (291 ± 19.9 fmol/mg) (Figure 4B); the K_d values ranged 2.35 ± 0.237 nM for ACh to 2.93 ± 0.205 nM for iperoxo. Control experiments at varying concentrations of orthosteric agonist (0, 10, 100, 1000 μM) were performed, and showed that no further co-operativity (increase in the B_{max}) was observed between 10 and 100 μM. This indicated that a lack of orthosteric binding site saturation was not the primary cause for the observed B_{max} differences. These results led us to hypothesize that the [³H]-LY2119620 binding was only reporting the G protein coupled active state-receptors (RG) population;

MOL #91751

thus changes in the receptor G protein coupling, here arising from differences in the efficiency of the orthosteric ligand to couple G protein, manifest as an apparent change in Bmax. To test whether similar receptor-G protein coupled affects could also be observed from the orthosteric site, experiments were repeated with the orthosteric radioligand. [³H]-Oxo-M.

Saturation binding experiments using [³H]-Oxo-M were performed in the presence of varying concentrations of the allosteric-site ligand LY2119620. Figure 4C and 4D shows a Bmax increase at the M₂ receptor from 793 ± 1.95 fmol/mg to 2850 ± 162 fmol/mg upon addition of 10 μM LY2119620 (Figure 4C); and about a 5-fold increase in Bmax at the M₄ receptor, 284 ± 18.3 fmol/mg to 1340 ± 42.2 fmol/mg (Figure 4D). The response was fully saturated at 10 μM LY2119620. The K_d values for the M₂ receptor are approximately 2 nM, and for the M₄ receptor decreases slightly from 3.27 ± 0.722 to 1.17 ± 0.185nM upon LY2119620 addition (Table 2). First, these Oxo-M studies verify that allosteric ligand binding modulates the orthosteric site binding. Second, these observations are consistent with the [³H]-LY2119620 binding data where Bmax predominantly changes upon ligand site occupation without a co-commitment change in ligand affinity (K_d).

To test the hypothesis that the change in Bmax being observed may reflect a G protein coupled active-state receptor pool the [³H]-Oxo saturation binding studies were repeated in the presence of the non-hydrolyzable guanine nucleotide GppNHp. Performing [³H]-Oxo experiments in the presence of GppNHp reduced the number of receptors in the active-RG state by uncoupling the G protein. Figure 4E and 4F, shows that [³H]-Oxo-M binding curve has an increase in Bmax from 721 ± 114nM to 1890 ± 271 nM when 1 μM LY2119620 was added, and that this increase was significantly reversed, Bmax of 995 ± 164 nM, by addition of GppNHp at the M₂ receptor (Figure 4E). Similar trends were observed at the M₄ receptor, however, the reversal was not seen to be as complete under the conditions tested (Figure 4F). Overall these saturation studies support the hypothesis that LY2119620 probe-dependence reflects an allosteric enhancement of the proportion of RG or G protein coupled active-state receptors.

[³H]-NMS competitive binding studies in the presence of LY2119620. As the equilibrium saturation studies failed to show an observable change in the K_d, a series of competitive binding experiments using [³H]-NMS were performed. This tested if the ability of the agonist iperoxo to compete with [³H]-NMS would change upon addition of LY2119620. Figure 4, shows that upon addition of the allosteric ligand, the dissociation rate of [³H]-NMS was retarded (Figure 5), although no overall changes, in the affinity of NMS for either the M₂ or M₄ receptors upon binding of the allosteric ligand LY2119620 were observed (Supplemental Figure 2). The magnitude of this dissociation rate affect varied with receptor-subtype. The dissociation rate of [³H]-NMS from the M₂ receptor in the presence of iperoxo was $0.347 \pm 0.0203 \text{ min}^{-1}$ and upon addition of LY2119620 slowed to $0.016 \pm 0.00790 \text{ min}^{-1}$ (Figure 5A); this relative change was very similar at the M₄ receptor (k_{off} reduced from $0.065 \pm 0.00160 \text{ min}^{-1}$ to $0.00938 \pm 0.00012 \text{ min}^{-1}$, Figure 5B). At the M₄ receptor the trends remained consistent with that observed at the M₂ receptor although the potency of LY2119620 was greater (Figure 5A-B); Table 3 summarizes all t_{1/2} and k_{off} rates for both the M₂ and M₄ receptors. Overall, these results are consistent with a model where LY2119620 is highly cooperative with orthosteric agonist binding, being more positively cooperative at the M₄ relative to M₂ receptor.

Additional [³H]-NMS displacement studies were performed to provide evidence that allosteric binding by LY2119620 could be observed to alter the binding affinity of the orthosteric ligand, reflected as a change in K_i of the agonist. Figure 5C and 5D show the competitive IC₅₀ value for iperoxo in the absence or presence of LY2119620, and shows that the IC₅₀ values for agonist competition of [³H]-NMS binding at both the M₂ and M₄ receptors increased significantly upon addition of LY2119620. Specifically, the K_i value of iperoxo reducing from $19.6 \pm 11.3 \text{ nM}$ to 0.732 ± 0.287 at the M₂ receptor; and from $15.1 \pm 3.40 \text{ nM}$ to $0.359 \pm 0.0366 \text{ nM}$ at the M₄ receptor (Figure 5C-D; for the K_d of [³H]-NMS in the presence of LY2119620 see Supplemental Figure 2). These [³H]-NMS data thus demonstrate that cooperativity between LY2119620 and orthosteric ligand sites can also be observed at the receptor-binding level (LY2119620 acts as a PAM).

Discussion

This study provides insight into the molecular pharmacology of the small molecule, LY2119620, which proves to be an M₂/M₄ receptor selective positive-allosteric modulator. Three major impacts of this work are: the identification of a novel M₂/M₄ receptor allosteric pharmacological tool that can be used to inform the development of treatments for neurological disorders such as schizophrenia; the exploration of probe dependence and the molecular mechanisms by which allosteric molecules may act upon a GPCR receptor and its signaling properties; and the characterization of the potent muscarinic-agonist iperoxo at the muscarinic M₂ and M₄ receptor and its modulation by an allosteric ligand.

The GTP- γ -S binding assays performed with LY2119620 demonstrate that LY2119620 displays modest allosteric agonism (Figure 2C) and positively modulates the functional G protein signaling ability of an agonist at the M₂/M₄ receptor subtypes (Figure 3). The degree of cooperativity between the orthosteric-allosteric ligands was found to vary depending on the agonist pairings, indicating probe-dependence. Probe-dependence for allosteric ligands has been reported before ((Gregory et al. 2010; Leach et al. 2010; Luttrell and Kenakin 2011; Suratman et al. 2011; Valant et al. 2012), see also the recent review by (Wootten et al. 2013)) and proves a significant challenge when trying to validate the suitability of a drug candidate. As the pharmacology can be dramatically impacted by this probe-dependence LY2119620 was evaluated with its natural agonist ACh, as well as full agonists Oxo-M and iperoxo. The results of the functional studies showed that LY2119620 enhanced the potency of all three agonists at the M₂ receptor: ACh 5-fold (34.3 ± 8.62 nM to 7.38 ± 2.03 nM); Oxo-M 10-fold (22.2 ± 3.51 nM to 2.04 ± 0.561 nM); and iperoxo 11-fold to a sub-nanomolar EC₅₀ of 71.1 ± 11.5 pM. At the M₄ receptor, the increase in potency was 22-fold for ACh (219 ± 42.8 nM to 10.0 ± 2.06 nM) and 47-fold for Oxo-M (123 ± 19.4 nM to 2.65 ± 1.05 nM); again the potency of iperoxo dropped to sub-nanomolar (EC₅₀=0.104 nM). Further exploration of whether these orthosteric-allosteric pairing effects seen in G protein signaling also manifest in other downstream signaling pathways such as ERK 1/2 phosphorylation, GSK3 β phosphorylation, and receptor internalization are being pursued in subsequent studies.

MOL #91751

The radioligand saturation binding studies presented in Figure 4 were performed to explore whether probe-dependence was also observed at the receptor-ligand binding level. The tritiated ligand, [³H]-LY2119620, allowed the binding of ACh, Oxo-M and iperoxo under identical experimental conditions. The results of these [³H]-LY2119620 studies showed that the number of allosteric receptor sites differed in an agonist-dependent manner, and that this change in B_{max} was not accompanied by a readily measurable change in K_d (Figure 4A and 4B). The lack of two-site binding curves indicated that LY2119620 wasn't binding to low and high-affinity receptor site populations. Hypothesizing that LY2119620 binding was only able to monitor the coupled active-state receptors (RG), the differences in B_{max} perhaps arose because the various orthosteric ligands had differential abilities to promote the receptors into the RG-state. Switching the radio-ligand to the orthosteric site, saturation binding studies were conducted with [³H]-Oxo-M in the presence of various concentrations of LY2119620 (Figure 4C-F). The [³H]-Oxo-M results suggest that LY2119620 binding to the allosteric site could also increase the number of orthosteric binding sites available (Figure 4C and 4D). Furthermore, Figure 4E and 4F showed that these allosteric-induced Oxo-M sites could be blocked by decoupling the G protein from the receptor (incubating the receptors with GppNHp) and shifting the receptor to a low-activity state. To summarize, the [³H]-Oxo-M saturation studies suggested that the allosteric ligand LY2119620 binds preferential to coupled active-state receptors, and can promote the number of receptors in this RG state. A similar redistribution of high- and low-affinity receptor sites was observed in a LY2033298, a congener M₄ receptor-PAM, study (Leach et al. 2010). Overall, the allosteric and orthosteric radioligand studies suggest that both Oxo-M and LY2119620 can place the M₂ and M₄ receptors into an active G protein bound state. Deeper insight into the complex interplay between the orthosteric, allosteric, and G protein coupled sites are now possible with the availability of tool compounds such as [³H]-LY2119620.

Additional radioligand studies were also performed to demonstrate that LY2119620 modulated the binding of agonists at the orthosteric site. Specifically, competitive binding experiments utilizing the [³H]-NMS radio-ligand demonstrated that LY2119620 binding at the allosteric site slowed the

MOL #91751

dissociation of NMS in the presence of the agonist iperoxo (Figure 4A-B). Additionally equilibrium [³H]-NMS saturation experiments showed that LY2119620 binding altered the affinity of iperoxo for the orthosteric site; the K_i for iperoxo decreased from 25.1 ± 14.5 nM to 0.878 ± 0.343 nM at the M₂ receptor (Figure 5 E-F). To summarize, these studies present experimental evidence that LY2119620 acts as a potent PAM for the M₄>M₂ receptor-subtypes as measured by both receptor binding (Figure 5) and G protein functional activity (Figure 3).

Another important result of this study was the characterization of the potent agonist, iperoxo, thus far described in the literature as an M₂-“super-agonist” (Kloeckner et al. 2010; Bock et al. 2012; Schrage et al. 2013) and its modulation by an allosteric ligand. Originating from screens for novel derivatives of Oxo-M (Dallanocce et al. 1999), iperoxo was found to possess both superior affinity and efficacy over ACh. Our work recapitulated previous findings that iperoxo possessed an EC₅₀ of 2.12 ± 0.0953 nM at the M₂ receptor (EC_{50(ACh)} / EC_{50(Iperoxo)} =56-fold, Figure 2A); and then expanded the pharmacological characterization to the M₄ receptor subtype and found similarly nanomolar potency (EC₅₀=8.47 ± 3.00 nM, and 61-fold enhancement in the EC_{50(ACh)} / EC_{50(Iperoxo)}, Figure 2B). Additionally the saturation binding and functional GTP-γ-S studies showed that this high efficacy agonist was able to be further modulated by binding of an allosteric compound (Figure 3 and 5).

This study of LY2119620 has explored the molecular mechanism of this M₂/M₄ receptor-subtype selective PAM mainly in a recombinant cellular system. Moreover, these studies corroborate and extend the initial characterization of the functional cooperativity observed between LY2119620 and iperoxo in [³H]-NMS binding, [³⁵S]-GTP-γ-S binding, and ERK 1/2 experiments (Kruse et al. 2013). The availability of a radio-labeled form of LY2119620, NMS, and Oxo-M ligands enabled the discovery that LY2119620 binding to the allosteric site increases the proportion of receptors in the G protein coupled active state. This insight may have implications in light of the emerging structural studies such as the recent active-state M₂ receptor crystal structure with iperoxo and LY2119620 docked in their respective binding sites (Kruse et al. 2013). While the crystal structure suggests that it is the entry of the orthosteric ligand which

MOL #91751

is critical for receptor movements leading to the appropriate unfolding of the intracellular domain region for G protein coupling, it is clear that the allosteric vestibule can also contribute to this switch to a permissive G protein binding state. Ultimately, our work in the development of the M₂/M₄ receptor-selective PAM, LY2119620, supports these crystallization efforts which provide the first atomic level understanding of such activation and allosteric modulation mechanisms of the muscarinic receptor family.

MOL #91751

Acknowledgments

We would like to acknowledge the labs of Dr. Christopoulos (Monash University) and Dr. Brian Kobilka (Stanford University) who contributed to both the successful development of this work, and the larger multi-national effort which generated the M2-active state crystal structure (4MQT) with the LY2119620 allosteric ligand bound.

MOL #91751

Authorship Contribution

Conducted experiments: Carrie H Croy, Doug Schober, and Hongling Xiao.

Contributed new reagents or analytic tools: Arthur Christopoulos

Performed data analysis: Carrie Croy, Arthur Christopoulos, Doug Schober, and Christian Felder.

Wrote or contributed to the writing of the manuscript: Carrie Croy, Christian Felder, Anne Quets, Doug Schober, and Arthur Christopoulos.

References

- Bock, A., N. Merten, R. Schrage, C. Dallanoce, J. Batz, J. Klockner, J. Schmitz, C. Matera, K. Simon, A. Kebig, L. Peters, A. Muller, J. Schrobang-Ley, C. Trankle, C. Hoffmann, M. De Amici, U. Holzgrabe, E. Kostenis and K. Mohr (2012). "The allosteric vestibule of a seven transmembrane helical receptor controls G-protein coupling." Nat Commun **3**: 1044.
- Bodick, N. C., W. W. Offen, A. I. Levey, N. R. Cutler, S. G. Gauthier, A. Satlin, H. E. Shannon, G. D. Tollefson, K. Rasmussen, F. P. Bymaster, D. J. Hurley, W. Z. Potter and S. M. Paul (1997). "Effects of xanomeline, a selective muscarinic receptor agonist, on cognitive function and behavioral symptoms in Alzheimer disease." Archives of Neurology **54**(4): 465-473.
- Brady, A. E., C. K. Jones, T. M. Bridges, J. P. Kennedy, A. D. Thompson, J. U. Heiman, M. L. Breininger, P. R. Gentry, H. Yin, S. B. Jadhav, J. K. Shirey, P. J. Conn and C. W. Lindsley (2008). "Centrally active allosteric potentiators of the M4 muscarinic acetylcholine receptor reverse amphetamine-induced hyperlocomotor activity in rats." J Pharmacol Exp Ther **327**(3): 941-953.
- Bridges, T. M., J. E. Marlo, C. M. Niswender, C. K. Jones, S. B. Jadhav, P. R. Gentry, H. C. Plumley, C. D. Weaver, P. J. Conn and C. W. Lindsley (2009). "Discovery of the first highly M5-preferring muscarinic acetylcholine receptor ligand, an M5 positive allosteric modulator derived from a series of 5-trifluoromethoxy N-benzyl isatins." J Med Chem **52**(11): 3445-3448.
- Bridges, T. M., C. M. Niswender, C. K. Jones, L. M. Lewis, C. D. Weaver, M. R. Wood, J. S. Daniels, P. J. Conn and C. W. Lindsley (2010). Discovery of a Highly Selective in vitro and in vivo M4 Positive Allosteric Modulator (PAM) Series with Greatly Improved Human Receptor Activity. Probe Reports from the NIH Molecular Libraries Program. Bethesda (MD).
- Bymaster, F. P., C. Felder, S. Ahmed and D. McKinzie (2002). "Muscarinic receptors as a target for drugs treating schizophrenia." Current Drug Targets CNS & Neurological Disorders **1**(2): 163-181.

MOL #91751

- Chan, W. Y., L. M. Broad, S. Lazareno, N. J. Birdsall, S. Bose, S. N. Mitchell, T. Large, R. Emkey, E. Sher, R. C. Thompson and C. C. Felder (2004). Pharmacological and molecular characterization of a positive allosteric modulator selective for muscarinic M4 receptor. Society for Neuroscience. San Diego, CA, 2004 Neuroscience Meeting Planner **Online**
- Chan, W. Y., D. L. McKinzie, S. Bose, S. N. Mitchell, J. M. Witkin, R. C. Thompson, A. Christopoulos, S. Lazareno, N. J. Birdsall, F. P. Bymaster and C. C. Felder (2008). "Allosteric modulation of the muscarinic M4 receptor as an approach to treating schizophrenia." Proc Natl Acad Sci U S A **105**(31): 10978-10983.
- Cheng, Y. and W. H. Prusoff (1973). "Relationship between the inhibition constant (K₁) and the concentration of inhibitor which causes 50 per cent inhibition (I₅₀) of an enzymatic reaction." Biochem Pharmacol **22**(23): 3099-3108.
- Christopoulos, A. and T. Kenakin (2002). "G protein-coupled receptor allosterism and complexing." Pharmacol Rev **54**(2): 323-374.
- Dallanocce, C., P. Conti, M. De Amici, C. De Micheli, E. Barocelli, M. Chiavarini, V. Ballabeni, S. Bertoni and M. Impicciatore (1999). "Synthesis and functional characterization of novel derivatives related to oxotremorine and oxotremorine-M." Bioorg Med Chem **7**(8): 1539-1547.
- Daval, S. B., E. Kellenberger, D. Bonnet, V. Utard, J. L. Galzi and B. Ilien (2013). "Exploration of the orthosteric/allosteric interface in human M1 muscarinic receptors by bitopic fluorescent ligands." Mol Pharmacol **84**(1): 71-85.
- DeLapp, N. W., J. H. McKinzie, B. D. Sawyer, A. Vandergriff, J. Falcone, D. McClure and C. C. Felder (1999). "Determination of [35S]guanosine-5'-O-(3-thio)triphosphate binding mediated by cholinergic muscarinic receptors in membranes from Chinese hamster ovary cells and rat striatum using an anti-G protein scintillation proximity assay." J Pharmacol Exp Ther **289**(2): 946-955.

MOL #91751

- Dencker, D., P. Weikop, G. Sorensen, D. P. Woldbye, G. Wortwein, J. Wess and A. Fink-Jensen (2012). "An allosteric enhancer of M(4) muscarinic acetylcholine receptor function inhibits behavioral and neurochemical effects of cocaine." Psychopharmacology (Berl) **224**(2): 277-287.
- Esteban, R. and D. Hillard. Thienopyridines as Allosteric Potentiators of the M4 Muscarinic Receptor. WO 2006/047124 A1 (May 2006).
- Felder, C. C., D. L. McKinzie, R. C. Thompson and B. L. Liu (2012). Muscarinic receptor agonists and positive allosteric modulators as novel mechanisms for the treatment of schizophrenia. Pharmacologic Treatments for Schizophrenia: Basics, Approaches, and Advances. W. M. and A. J.S. NY, Wiley.
- Gannon, R. L. and M. J. Millan (2012). "LY2033298, a positive allosteric modulator at muscarinic M(4) receptors, enhances inhibition by oxotremorine of light-induced phase shifts in hamster circadian activity rhythms." Psychopharmacology (Berl) **224**(2): 231-240.
- Gregory, K. J., N. E. Hall, A. B. Tobin, P. M. Sexton and A. Christopoulos (2010). "Identification of orthosteric and allosteric site mutations in M2 muscarinic acetylcholine receptors that contribute to ligand-selective signaling bias." J Biol Chem **285**(10): 7459-7474.
- Huang, X. P., S. Prilla, K. Mohr and J. Ellis (2005). "Critical amino acid residues of the common allosteric site on the M2 muscarinic acetylcholine receptor: more similarities than differences between the structurally divergent agents gallamine and bis(ammonio)alkane-type hexamethylene-bis-[dimethyl-(3-phthalimidopropyl)ammonium]dibromide." Mol Pharmacol **68**(3): 769-778.
- Huynh, T., C. Valant, I. T. Crosby, P. M. Sexton, A. Christopoulos and B. Capuano (2013). "Probing Structural Requirements of Positive Allosteric Modulators of the M Muscarinic Receptor." J Med Chem. **56**(20): 8196-8200.

MOL #91751

- Jones, C. K., N. Byun and M. Bubser (2012). "Muscarinic and nicotinic acetylcholine receptor agonists and allosteric modulators for the treatment of schizophrenia." Neuropsychopharmacology **37**(1): 16-42.
- Kenakin, T. (2007). "Functional selectivity through protean and biased agonism: who steers the ship?" Mol Pharmacol **72**(6): 1393-1401.
- Kloeckner, J., J. Schmitz and U. Holzgrabe (2010). "Convergent, short synthesis of the muscarinic superagonist iperoxo." Tetrahedron Letters **51**: 3470-2472.
- Kruse, A. C., A. M. Ring, A. Manglik, J. Hu, K. Hu, K. Eitel, H. Hubner, E. Pardon, C. Valant, P. M. Sexton, A. Christopoulos, C. C. Felder, P. Gmeiner, J. Steyaert, W. I. Weis, K. C. Garcia, J. Wess and B. K. Kobilka (2013). "Activation and allosteric modulation of a muscarinic acetylcholine receptor." Nature **504**: 101-106.
- Langmead, C. J. and A. Christopoulos (2013). "Supra-physiological efficacy at GPCRs: superstition or super agonists?" Br J Pharmacol **169**(2): 353-356.
- Le, U., B. J. Melancon, T. M. Bridges, P. N. Vinson, T. J. Utley, A. Lamsal, A. L. Rodriguez, D. Venable, D. J. Sheffler, C. K. Jones, A. L. Blobaum, M. R. Wood, J. S. Daniels, P. J. Conn, C. M. Niswender, C. W. Lindsley and C. R. Hopkins (2013). "Discovery of a selective M(4) positive allosteric modulator based on the 3-amino-thieno[2,3-b]pyridine-2-carboxamide scaffold: development of ML253, a potent and brain penetrant compound that is active in a preclinical model of schizophrenia." Bioorg Med Chem Lett **23**(1): 346-350.
- Leach, K., A. E. Davey, C. C. Felder, P. M. Sexton and A. Christopoulos (2011). "The role of transmembrane domain 3 in the actions of orthosteric, allosteric, and atypical agonists of the M4 muscarinic acetylcholine receptor." Mol Pharmacol **79**(5): 855-865.
- Leach, K., R. E. Loiacono, C. C. Felder, D. L. McKinzie, A. Mogg, D. B. Shaw, P. M. Sexton and A. Christopoulos (2010). "Molecular mechanisms of action and in vivo validation of an M4

MOL #91751

muscarinic acetylcholine receptor allosteric modulator with potential antipsychotic properties."

Neuropsychopharmacology **35**(4): 855-869.

Lewis, L. M., T. M. Bridges, C. M. Niswender, C. D. Weaver and C. W. Lindsley (2010). Discovery of a Highly Selective in vitro and in vivo M4 Positive Allosteric Modulator (PAM). Probe Reports from the NIH Molecular Libraries Program. Bethesda (MD).

Luttrell, L. M. and T. P. Kenakin (2011). "Refining efficacy: allosterism and bias in G protein-coupled receptor signaling." Methods Mol Biol **756**: 3-35.

McKinzie, D. L. and F. P. Bymaster (2012). "Muscarinic mechanisms in psychotic disorders." Handb Exp Pharmacol(213): 233-265.

Nawaratne, V., K. Leach, C. C. Felder, P. M. Sexton and A. Christopoulos (2010). "Structural determinants of allosteric agonism and modulation at the M4 muscarinic acetylcholine receptor: identification of ligand-specific and global activation mechanisms." J Biol Chem **285**(25): 19012-19021.

Nawaratne, V., K. Leach, N. Suratman, R. E. Loiacono, C. C. Felder, B. N. Armbruster, B. L. Roth, P. M. Sexton and A. Christopoulos (2008). "New insights into the function of M4 muscarinic acetylcholine receptors gained using a novel allosteric modulator and a DREADD (designer receptor exclusively activated by a designer drug)." Mol Pharmacol **74**(4): 1119-1131.

Salovich, J. M., P. N. Vinson, D. J. Sheffler, A. Lamsal, T. J. Utley, A. L. Blobaum, T. M. Bridges, U. Le, C. K. Jones, M. R. Wood, J. S. Daniels, P. J. Conn, C. M. Niswender, C. W. Lindsley and C. R. Hopkins (2012). "Discovery of N-(4-methoxy-7-methylbenzo[d]thiazol-2-yl)isonicotinamide, ML293, as a novel, selective and brain penetrant positive allosteric modulator of the muscarinic 4 (M4) receptor." Bioorg Med Chem Lett **22**(15): 5084-5088.

Schober, D. A., C. H. Croy, H. Xiao, A. Christopoulos and C. C. Felder (submitted). "Development of an allosteric radiotracer, [3H]-LY2119620, to monitor human Muscarinic Acetylcholine Receptors".

MOL #91751

- Schrage, R., W. K. Seemann, J. Klockner, C. Dallanoce, K. Racke, E. Kostenis, M. De Amici, U. Holzgrabe and K. Mohr (2013). "Agonists with supraphysiological efficacy at the muscarinic M2 ACh receptor." Br J Pharmacol **169**(2): 357-370.
- Shekhar, A., W. Z. Potter, J. Lightfoot, J. Lienemann, S. Dube, C. Mallinckrodt, F. P. Bymaster, D. L. McKinzie and C. C. Felder (2008). "Selective muscarinic receptor agonist xanomeline as a novel treatment approach for schizophrenia." Am J Psychiatry **165**(8): 1033-1039.
- Shirey, J. K., Z. Xiang, D. Orton, A. E. Brady, K. A. Johnson, R. Williams, J. E. Ayala, A. L. Rodriguez, J. Wess, D. Weaver, C. M. Niswender and P. J. Conn (2008). "An allosteric potentiator of M4 mAChR modulates hippocampal synaptic transmission." Nat Chem Biol **4**(1): 42-50.
- Suratman, S., K. Leach, P. Sexton, C. Felder, R. Loiacono and A. Christopoulos (2011). "Impact of species variability and 'probe-dependence' on the detection and in vivo validation of allosteric modulation at the M4 muscarinic acetylcholine receptor." Br J Pharmacol **162**(7): 1659-1670.
- Valant, C., C. C. Felder, P. M. Sexton and A. Christopoulos (2012). "Probe dependence in the allosteric modulation of a G protein-coupled receptor: implications for detection and validation of allosteric ligand effects." Mol Pharmacol **81**(1): 41-52.
- Wess, J. (2012). "Novel muscarinic receptor mutant mouse models." Handb Exp Pharmacol(208): 95-117.
- Wess, J., R. M. Eglén and D. Gautam (2007). "Muscarinic acetylcholine receptors: mutant mice provide new insights for drug development." Nat Rev Drug Discov **6**(9): 721-733.
- Wooten, D., A. Christopoulos and P. M. Sexton (2013). "Emerging paradigms in GPCR allostery: implications for drug discovery." Nat Rev Drug Discov **12**(8): 630-644.
- Young, J. W., X. Zhou and M. A. Geyer (2010). "Animal models of schizophrenia." Curr Top Behav Neurosci **4**: 391-433.

Figure Legends

Figure 1: The structure of the pharmacological compound LY2119620. The chemical structure of the M₂/M₄ receptor subtype-selective allosteric modulator LY2119620.

Figure 2: Functional agonism of the M₂ and M₄ receptors measured using [³⁵S] GTP-γ S binding.

Functional G protein activation upon orthosteric ligand binding was measured at the M₂ and M₄ receptors. Data were processed by subtracting out the background (signal in absence of agonist) and then normalizing to the acetylcholine response at 100 μM agonist. Minimal functional agonism was observed for LY2119620 at the M₁, M₃, and M₅ receptor subtypes (<20%, See Supplemental Figure 1). **A-B.** These agonist response curves were collected to show the potency of iperoxo at the M₂ and M₄ receptors. The agonist response curves for ACh (○), iperoxo (●), Oxo-M (□), and McN-A-343 (△). **A.** The EC₅₀ values at the M₂ receptor were 2.12 ± 0.0953 nM for Iperoxo, 68.0 ± 18.3 nM for Oxo, 118 ± 32 nM for ACh, and 2650 ± 139 for McN-A-343. **B.** The EC₅₀ values at the M₄ receptor were 8.47nM ± 3.0 0 nM for Iperoxo, 231 ± 34.6nM for Oxo, 514 ± 22.0 nM for ACh, and 1190 ± 56.1 nM for McN-A-343. **C.** Additional GTP-γ-S binding assays were used to measure whether LY2119620 showed allosteric agonism (activity in the absence of orthosteric ligand). An agonist response curve for LY2119620 in the absence of non-endogenous orthosteric compound was measured at the M₂ (○) and M₄ receptor (□); this data was normalized to the maximal-ACh response at these receptors, M₂ (●) and M₄ (■). Data curves presented are the means ± SEM of three independent experiments conducted in duplicate.

Figure 3: [³⁵S] GTP-γS binding at the M₂ and M₄ receptors in the presence of LY2119620.

G-protein coupled activity for M₁-M₅AChR receptors were tested in the presence of orthosteric ligands, ACh, Oxo-M or ipreoxo, and varying concentrations of LY2119620. No shifts in the binding curves were observed for the M₁, M₃ or M₅ receptor subtypes (See Supplemental Figure 1). All binding curves were normalized to the maximal response of the orthosteric ligand (denoted on the x-axis), 100 μM ACh or Oxo-M or 0.1 μM iperoxo. The binding curves are color coded by LY2119620 present with 10 μM (red), 3 μM

MOL #91751

(orange), 1 μ M (yellow), 0.4 μ M (green), 0.1 μ M (blue), 0.04 μ M (grey), or 0 μ M (black) LY2119620. **A.** The GTP- γ -S binding curves of ACh at the M_2 receptor. **B.** The GTP- γ -S binding curves of ACh at the M_4 receptor with LY2119620 **C.** The GTP- γ -S binding curves of Oxo-M at the M_2 receptor with LY2119620 **D.** The GTP- γ -S binding curves of Oxo-M at the M_4 receptor with LY2119620 **E.** The GTP- γ -S binding curves of iperoxo at the M_2 receptor **F.** The GTP- γ -S binding curves of Iperoxo at the M_4 receptor. Data curves presented are the means \pm SEM of three to four independent experiments in duplicate.

Figure 4: Orthosteric and allosteric radio-ligand saturation binding studies at the M_2 and M_4 receptors. **A-B.** Saturation binding experiments using the allosteric radioligand [3 H]-LY2119620 in the presence of various orthosteric agonists (100 μ M ACh, Oxo-M, or iperoxo) were measured at M_1 - M_5 . The M_1 , M_3 , M_5 receptor subtypes showed no detectable specific binding. The graphs represent the equilibrium binding of [3 H]-LY2119620 (1 hour, 25 $^{\circ}$ C incubation) with 100 μ M orthosteric ligands, ACh (O), Oxo-M (□) or iperoxo (●) at the **A.** M_2 - or **B.** M_4 receptor. **C-D.** Saturation binding experiments using the orthosteric ligand [3 H]-Oxo-M were carried out in the presence of multiple concentrations of LY2119620 under equilibrium conditions (30m incubation at 25 $^{\circ}$ C). The graphs present the specific binding signal of [3 H]-Oxo-M in the presence of 0 (O), 0.1 (▲), 1 (■), or 10(●) μ M LY2119620 at the **C.** M_2 **D.** M_4 receptors. **E-F.** [3 H]-Oxo saturation binding curves in the presence of LY2119620 and GppNHp. [3 H]-Oxo-M binding to the M_2 and M_4 receptor-expressing membranes was allowed reach equilibrium (30mins at 25 $^{\circ}$ C) in the presence of GppNHp prior to the addition LY2119620. The graphs show the specific binding [3 H]-Oxo-M with membranes alone (●), membranes and 10 μ M LY2119620 (■), or membranes with 100 μ M LY2119620 and 100 μ M GppNHp (▲) at the **(A)** M_2 and **(B)** M_4 receptor. Data curves presented are the means \pm SEM of three to six independent experiments conducted in duplicate.

Figure 5: [3 H]-NMS kinetic and equilibrium studies in the presence of LY2119620 **A-B.** The dissociation rates of [3 H]-NMS being displaced by agonist iperoxo in the presence of LY2119620 were

MOL #91751

determined by capturing 1-90min time points in an end-point assay. The competing agonist was added after [³H]-NMS reached binding equilibrium (60 min at 25 ° C) with the M₂/M₄AChR- membranes and LY2119620. **A.** The kinetic dissociation curves show the displacement of [³H]-NMS at the M₂ receptor by 10 μM iperoxo in the presence of 0 (●), 10 (◇), 20 (△) or 40 μM (□) LY2119620. **B.** The kinetic dissociation curves show the displacement of [³H]-NMS by 10 μM iperoxo at the M₄ receptor in the presence of 0 (●), 5 (○), 10 (◇) or 20 μM (△) LY2119620. **C-D.** These panels show the displacement of [³H]-NMS under equilibrium conditions by 100 μM iperoxo in the presence of 0 (●) or 10μM (■) LY2119620 at the **C.** M₂ or **D.** M₄ receptor. The equilibrium experiment allows the quantification of the potency change in iperoxo, IC₅₀ and/or K_i, upon LY2119620 binding. **A-D.** Data curves presented are the means ± SEM of three independent experiments conducted in duplicate.

MOL #91751

Table 1: Changes in the agonist EC₅₀ upon addition of LY2119620. The change in the EC₅₀ value of agonists ACh, Oxo-M, and iperexo upon addition of the allosteric ligand, LY2119620, were measured using a G-protein coupled functional assay. Values presented represent the means ± SEM of three independent experiments conducted in duplicate.

EC ₅₀ (nM)	Agonist Alone	LY2119620 [10μM]	LY2119620 [3μM]	LY2119620 [1μM]	LY2119620 [0.4μM]	LY2119620 [0.1μM]	LY2119620 [0.04μM]
Ach at M ₂	34.3 ± 8.62	7.38 ± 2.03	10.1 ± 3.36	23.1 ± 4.85	34.1 ± 19.7	41.2 ± 1.58	27.8 ± 8.49
Ach at M ₄	219 ± 42.8	10.0 ± 2.06	13.5 ± 5.03	31.6 ± 22.3	51.5 ± 30.0	80.6 ± 18.3	101 ± 19.0
Oxo-M at M ₂	22.2 ± 3.51	2.04 ± 0.561	0.956 ± 0.104	1.57 ± 0.270	4.58 ± 1.03	8.14 ± 1.89	11.1 ± 0.0740
Oxo-M at M ₄	123 ± 19.4	2.65 ± 1.05	2.45 ± 0.0758	2.99 ± 1.03	7.36 ± 1.94	15.6 ± 4.61	30.3 ± 9.00
iperexo at M ₂	0.736 ± 0.192	0.0711 ± 0.0115	0.0532 ± 0.00594	0.0786 ± 0.0101	0.197 ± 0.0582	0.617 ± 0.0386	0.827 ± 0.469
iperexo at M ₄	0.300 ± 0.0470	0.104 ± 0.00607	0.0925 ± 0.00529	0.0942 ± 0.00737	0.164 ± 0.00766	0.230 ± 0.0185	0.244 ± 0.0183

MOL #91751

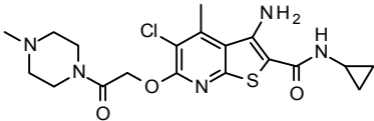
Table 2: Binding of [³H]-Oxo-M to the M₂ and M₄ receptors in the presence of varying concentrations of LY2119620. Membranes were incubated with [3H]-Oxo-M with various concentrations of LY2119620 (0, 0.1, 1, 10 μM) for 30 minutes at room temperature. Data shown are the result of three independent experiments performed in duplicate.

	0 μM LY2119620		0.1 μM LY2119620		1 μM LY2119620		10 μM LY2119620	
	Bmax (fmol/mg)	Kd (nM)	Bmax (fmol/mg)	Kd (nM)	Bmax (fmol/mg)	Kd (nM)	Bmax (fmol/mg)	Kd (nM)
M₂ receptor	793 ± 1.95	1.89 ± 0.510	1410 ± 230	1.71 ± 0.653	1830 ± 468	1.38 ± 0.134	2850 ± 162	2.16 ± 0.729
M₄ receptor	284 ± 18.3	3.27 ± 0.722	960 ± 83.8	1.91 ± 0.454	889 ± 191	1.24 ± 0.204	1340 ± 42.2	1.17 ± 0.185

Table 3: Displacement of [³H]-NMS by orthosteric ligands in the presence of LY2119620 at the M₂ and M₄ receptors. [³H]-NMS dissociation kinetic binding assays performed in the presence of varying concentrations of LY2119620 (0-40 μM) at the M₂ and M₄ receptors. Receptors were incubated with [³H]-NMS for 1 hour at 30 °C; once equilibrated, 1 μM iperexo was added in a time-staggered approach to capture 1-90 minute time-points. The specific binding data was fit to a single exponential decay to calculate the dissociation rate constants (min⁻¹) reported. Data shown are the result of three independent experiments performed in duplicate.

M ₂	0 μM LY2119620		40 μM LY2119620		20 μM LY2119620		10 μM LY2119620	
	t _{1/2} (min)	k _{off} (min ⁻¹)	t _{1/2} (min)	k _{off} (min ⁻¹)	t _{1/2} (min)	k _{off} (min ⁻¹)	t _{1/2} (min)	k _{off} (min ⁻¹)
Iperoxo	2.01 ± 0.125	0.347 ± 0.0203	36.9 ± 14.7	0.016 ± 0.00790	12.2 ± 2.70	0.0616 ± 0.011	5.59 ± 0.466	0.126 ± 0.0102
M ₄	0 μM LY2119620		20 μM LY2119620		10 μM LY2119620		5 μM LY2119620	
	t _{1/2} (min)	k _{off} (min ⁻¹)	t _{1/2} (min)	k _{off} (min ⁻¹)	t _{1/2} (min)	k _{off} (min ⁻¹)	t _{1/2} (min)	k _{off} (min ⁻¹)
Iperoxo	10.6 ± 0.257	0.065 ± 0.00160	73.9 ± 0.945	0.00938 ± 0.00012	30.6 ± 5.12	0.0242 ± 0.00450	20.0 ± 3.12	0.0365 ± 0.00587

Figure 1



LY2119620

Figure 2

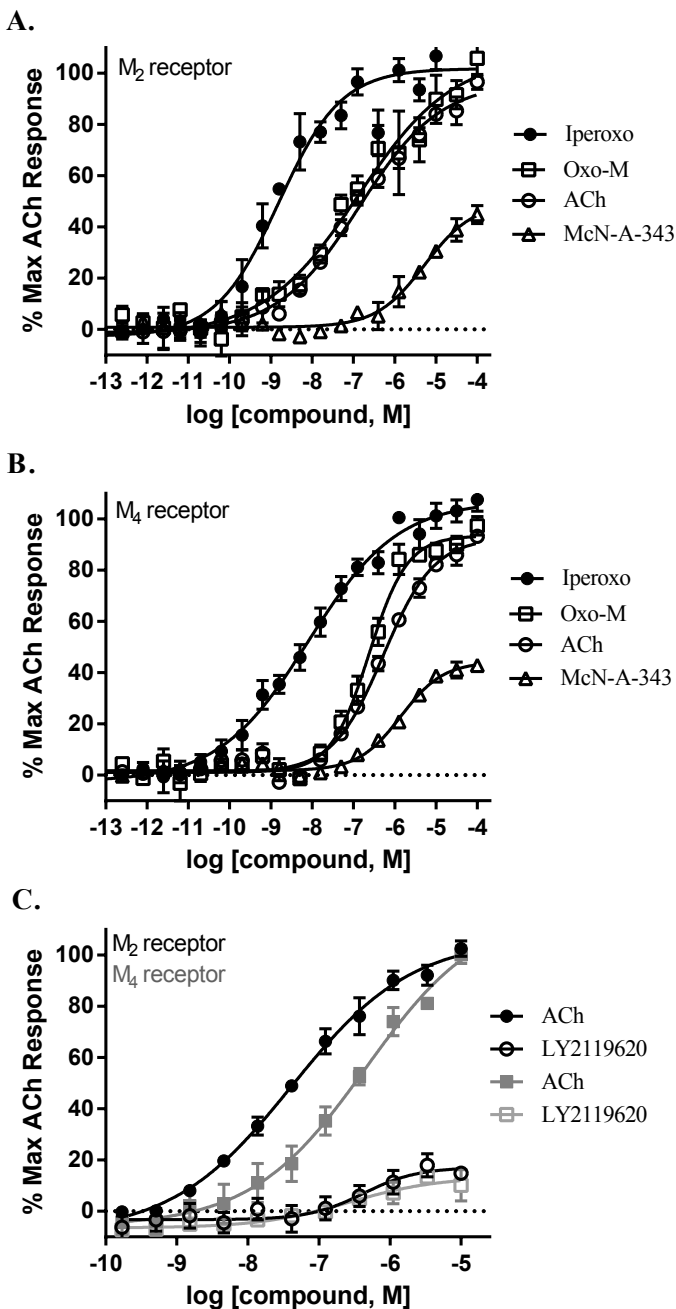
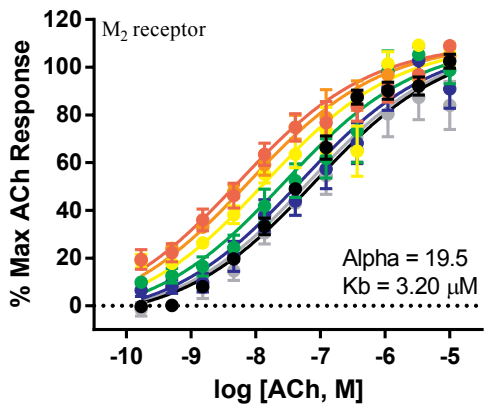
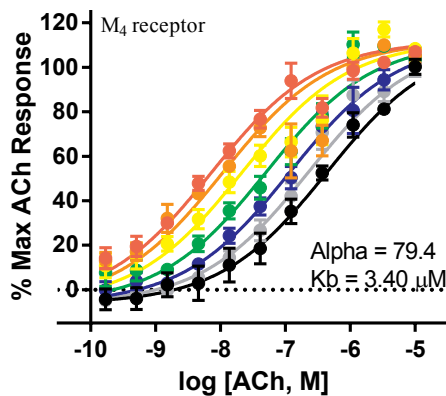


Figure 3

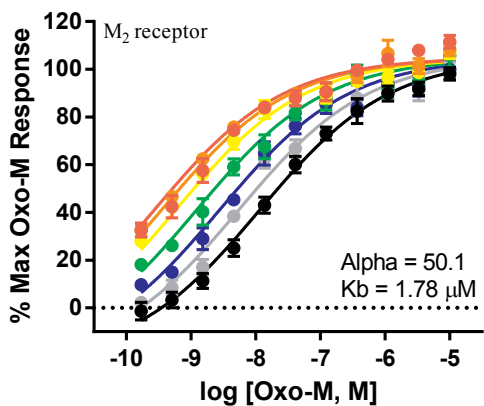
A.



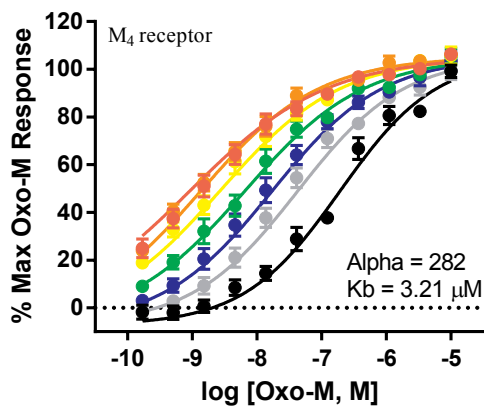
B.



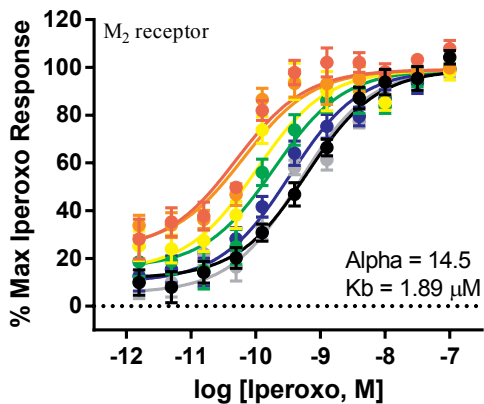
C.



D.



E.



F.

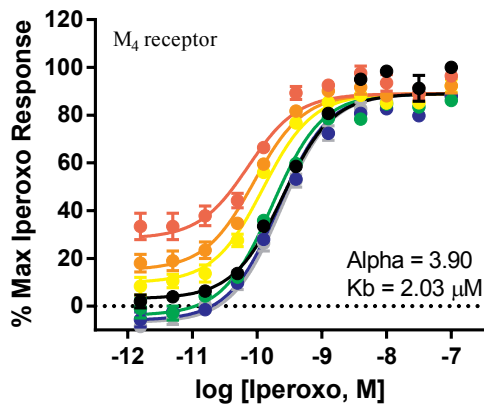
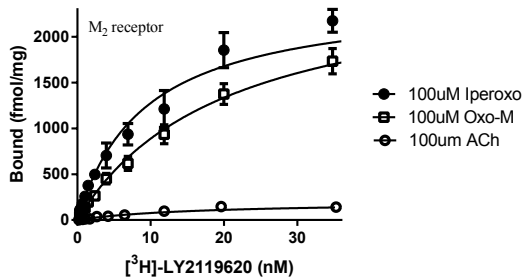
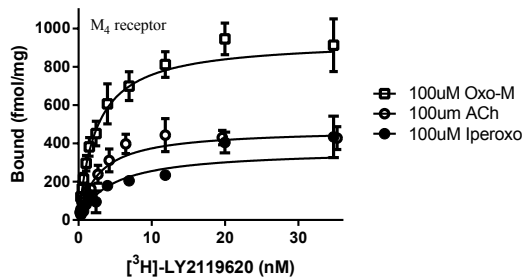


Figure 4

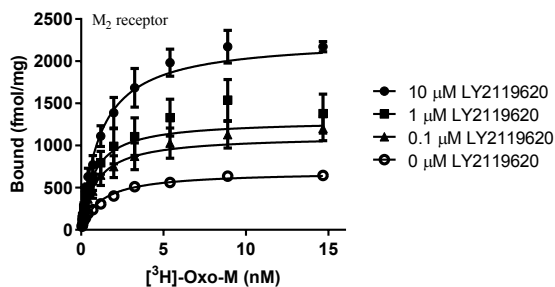
A.



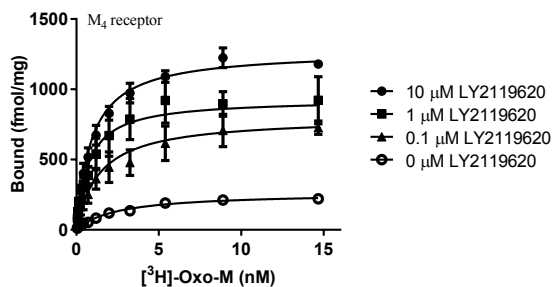
B.



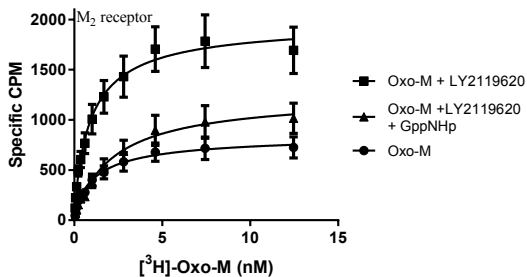
C.



D.



E.



F.

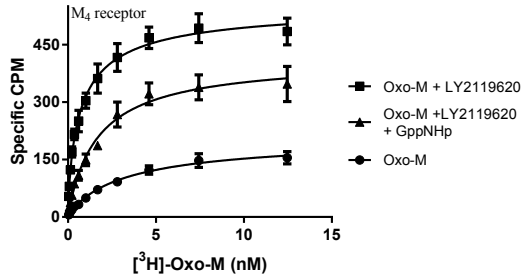
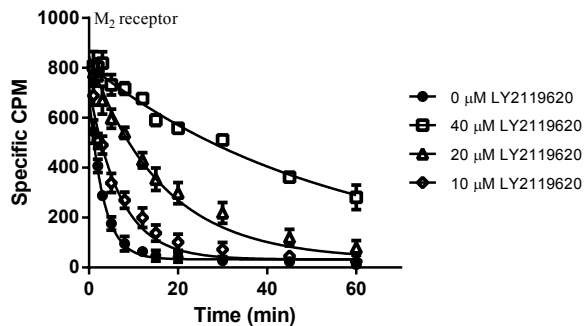
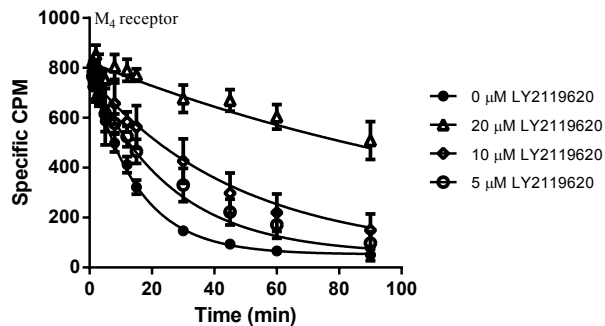


Figure 5

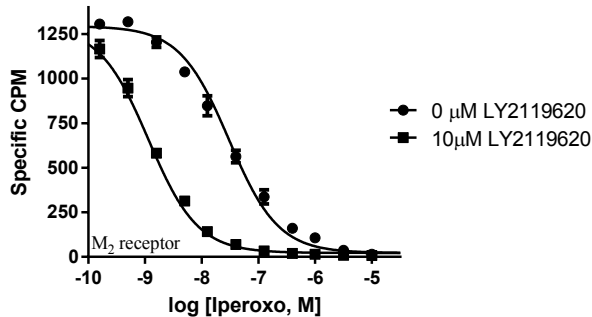
A.



B.



C.



D.

